RESEARCH ARTICLE

High gestational leucine level dampens WDPCP/MAPK signaling to impair the EMT and migration of cardiac microvascular endothelial cells in congenital heart defects

Wei Hong | **Guozhou You** | **Zhongming Luo** | **Mingxiang Zhang** | **Jian Chen** (ID)

Kunming Children's Hospital, Kunming, Yunnan, China

Correspondence
Jian Chen, No. 288 Qianxing Rd, Kunming, 650034, Yunnan, China.
Email: chenjian7@kmmu.edu.cn

Abstract

Congenital heart defects (CHDs) represent one of the most prevalent categories of neonatal defects, and maternal dietary patterns have been linked to the risk of these conditions. Branched-chain amino acids (BCAAs), particularly leucine, are essential for various metabolic and physiological processes involved in heart development. In this study, we examined the molecular mechanisms through which elevated levels of leucine induce defects in cardiac microvascular endothelial cells. We collected plasma samples from healthy controls and neonatal patients with CHDs, employed a high-leucine diet for pregnant female mice, and applied high-leucine treatment in human cardiac microvascular endothelial cells (HCMECs). The impacts of high-leucine levels on WD Repeat Containing Planar Cell Polarity Effector (WDPCP)/MAPK signaling axis were investigated in the cell and animal models. We reported heightened plasma leucine levels in neonatal patients with CHDs and observed that a high-leucine diet in pregnant mice was associated with reduced expression of WDPCP and attenuated MAPK/ERK signaling. High-leucine treatment in HCMECs impaired epithelial-mesenchymal transition (EMT) and cell migration; however, overexpression of WDPCP or activation of MAPK exhibited a rescue effect. The upregulation of endomucin (EMCN) under high-leucine conditions contributed to the impaired EMT and migratory capacity of HCMECs, and the WDPCP/MAPK signaling axis regulated EMCN overexpression in response to high-leucine treatment. High levels of leucine in neonatal patients with CHDs may inhibit the WDPCP/MAPK axis, leading to an increase in EMCN expression that undermines the function of cardiac microvascular endothelial cells. These findings suggest the potential of targeting the WDPCP/MAPK axis as an intervention strategy for neonatal CHDs.

KEYWORDS
congenital heart defects (CHDs), EMCN, leucine, MAPK/ERK, WDPCP

Wei Hong contributed equally to this study.

INTRODUCTION

Congenital heart defects (CHDs) are one of the most prevalent types of neonatal anomalies, with an estimated prevalence of up to 1% (8 to 10 per 1000 live births, ranging from 0.8% to 1%).[1] Many neonatals with CHDs are diagnosed after birth through the observation of symptoms or medical screening. However, for those who remain undiagnosed until after hospital discharge, the risk of critical cardiac lesions and mortality significantly increases without timely intervention.[2,3] Increasing evidence highlights the critical influence of maternal health conditions on the risk of CHDs. For instance, smoking, exposure to secondhand smoke, inappropriate medication use during the first trimester of pregnancy, diabetes, and phenylketonuria are all strongly associated with neonatal CHDs.[4–7] Additionally, maternal diet plays a significant role in fetal development, as poor maternal nutrition during pregnancy is a major contributor to birth defects. Specifically, low intake of iron and folate is strongly linked to an increased risk of CHDs.[8,9] Fetuses of women following a vegetarian diet have a higher likelihood of developing CHDs, whereas newborns of pregnant women with high dairy and egg consumption exhibit a reduced risk of CHDs.[10] Furthermore, dietary supplementation with multivitamins has been reported to offer protection against neonatal CHDs.[11]

Branched-chain amino acids (BCAAs), including leucine and isoleucine, are abundant in plasma and essential for various metabolic and physiological functions related to heart development.[12] Leucine supplementation has been reported to exert a protective effect against cardiovascular defects.[12–14] However, a recent study indicated that abnormally high plasma levels of leucine during the first trimester were significantly associated with an increased risk of CHDs in offspring, a finding corroborated in pregnant mice fed a high-leucine diet.[15] Nonetheless, the mechanisms through which elevated levels of leucine influence the cardiovascular system and their effects on cardiac microvascular endothelial cells remain largely unexplored.

WD Repeat Containing Planar Cell Polarity Effector (WDPCP) is a protein that regulates the septin cytoskeletal structure in collective cell movement and ciliogenesis.[16] WDPCP has also been implicated in limb development by modulating cell growth and differentiation.[17] Given that planar cell polarity is essential for cardiac morphogenesis, heart tube remodeling, and the angiogenesis of endothelial cells,[18–21] WDPCP may play a role in cardiac development. Indeed, evidence suggests that WDPCP mediates epicardial epithelial-mesenchymal transition (EMT) and cardiac cell migration during coronary artery remodeling.[22] However, the potential involvement of WDPCP dysregulation in the progression of CHDs remains to be investigated.

In the current study, we investigated the impacts of a high-leucine diet on neonatal CHDs and the expression of WDPCP. We also dissected the molecular mechanism by which WDPCP dysregulation, induced by high-levels of leucine, triggers defects in cardiac microvascular endothelial cells. Our findings showed that a high-leucine diet in pregnant mice caused a reduction in WDPCP expression and dampened the signaling activity of the mitogen-activated protein kinase (MAPK)/extracellular signal-regulated kinase (ERK) axis. This contributed to an overexpression of endomucin (EMCN), which impairs the EMT and the migratory capacity of cardiac microvascular endothelial cells. Together, our data suggest that elevated leucine levels induce the downregulation of WDPCP, and the consequent upregulation of EMCN impairs the function of cardiac microvascular endothelial cells.

MATERIALS AND METHODS

Clinical samples

The blood samples from age and sex-matched healthy controls and infants diagnosed with congenital heart disease (CHD) were collected in Kunming Children's Hospital. All the recruited subjects were male and 10 months old, and the family did not have a historical record of coronary artery disease. The diagnosis of CHD in the neonatals was based on electrocardiogram, echocardiogram, cardiac catheterization, and angiogram and cardiac CT scan, based on the previous guidelines.[23,24] The blood samples were immediately frozen in liquid nitrogen before further analysis. The usage of human samples was approved by the Medical Ethics Committee of Kunming Children's Hospital (2021-03-340-K01). The parents of all the recruited subjects signed the informed consent.

Cell culture

Human cardiac microvascular endothelial cells (HCMECs) were purchased from ScienCell (Catalog #0.6000; supplier: Hengya Biotech). The cells were authenticated through STR profiling and tested to be mycoplasma-free by the supplier. HCMECs were

cultured in VascuLife® EnGS-Mv Medium (LL-0004, Lifeline Cell Technology). For leucine supplementation, L-Leucine (Cell culture grade, J62824.22, ThermoFisher Scientific) was added to the culture medium at a final concentration of 2 mM. The formulated commercial culture medium contains 0.8 mM leucine, and the high-leucine condition contains 2.5 times of the leucine level in the original culture medium. This level of leucine increase is in line with the elevation observed in the clinical samples and the leucine overfeeding animal model of this study, and is also consistent with the previously reported plasma leucine level increase in obese mice.[25] Before functional experiment or molecular analysis, HCMECs were cultured in standard or high-leucine medium for 48 h. For MAPK activation, cells were treated with 1 μM C16-PAF (HY-108635, MedChemExpress).

Cell transfection

To overexpress WDPCP, the complementary DNA (cDNA) sequence of WDPCP was cloned into the pcDNA-3.1 expression vector by RiboBio. For EMCN knockdown, control small interfering RNA (siRNA, si-NC) and EMCN siRNA (si-EMCN) were produced by GenePharma (Shanghai, China). Sequences for si-NC: 21nt guide (5′ → 3′): UUAGCAUAUUACUUUGUAGCC, 21nt passenger (5′ → 3′): CUACAAAGUAAUAUGCUAAUC. Sequences for si-EMCN: 21nt guide (5′ → 3′): AAAAGUAGCUGUUGACAUCAG, 21nt passenger (5′ → 3′): GAUGUCAACAGCUACUUUUUU. Lipofectamine 3000 kit (L3000015, Invitrogen) was adopted for cellular transfection. Five micrograms plasmid or 100 nM of siRNA was used for transfecting cells in six-well plates. Cells were seeded with a density of 5×10^5 cells per well. The molecules were mixed with 150 μL Opti-MEM® I Reduced-Serum Medium (11058021, ThermoFisher Scientific), and then 6 μL Lipofectamine 3000 reagent was added and the mixture was incubated for 15 min. Forty-eight hours after the transfection, cells were collected for further analysis.

Wound healing assay

HCMECs were cultivated in a 12-well plate to achieve 80% confluence. A sterile pipette tip was used to make a wound line in the middle region of the cell monolayer, and the medium was changed to eliminate the floating cells. The plates were placed back to 37°C and incubated for 48 h. The images of cell culture were recorded using a light microscope (Leica AM6000 microscope, Leica).

Transwell invasion assay

The 24-well transwell chambers, loaded with Matrigel (356237, Corning), were utilized in the Transwell invasion assay. Following the specified treatment, the cells were harvested via trypsinization and re-suspended in a serum-free medium. The cell density was adjusted to 2.5×10^5 cells/mL. The lower compartment was filled with 500 μL of medium containing 20% fetal bovine serum, while 500 μL of the cell suspension was added to the apical chamber. The plate was returned to the incubator, and the cells were cultivated at 37°C for 18 h. Subsequently, the cells adjacent to the lateral membrane of the apical chamber were wiped away. The remaining cells were fixed with 4% paraformaldehyde and stained with 0.25% crystal violet (C0121, Beyotime) for 20 min at ambient temperature. Stained cells were then observed at 200× magnification, and five random visual fields were recorded for cell counting in each condition.

CCK-8 cell proliferation assay

Cell proliferation was assessed using the Cell Counting Kit-8 (CCK-8) assay (Beyotime Biotechnology, Shanghai, China; Cat. No. C0037) in accordance with the manufacturer's instructions. Briefly, cells were seeded in 96-well plates at a density of 5×10^3 cells per well and cultured for 24 h. Following treatment, 10 μL of CCK-8 solution was added to each well containing 100 μL of culture medium. The plates were then incubated for 1 to 4 h at 37°C in a humidified atmosphere with 5% CO_2. Absorbance was measured at 450 nm using a microplate reader (SpectraMax M5, Molecular Devices). Cell viability was calculated as a percentage relative to the untreated control group. All experiments were conducted in triplicate.

Western blot

Protein contents were isolated from cells or plasma samples using a Radioimmunoprecipitation assay buffer (RIPA buffer) containing the protease inhibitor cocktail (78429, ThermoFisher Scientific). The protein concentration was then quantified using a Bicinchoninic Acid (BCA) assay kit (P0012, Beyotime). A total of 5 μg protein sample was denatured and subsequently analyzed in a 12% polyacrylamide gel. The separated bands were transferred from the polyacrylamide gel to a polyvinylidene difluoride (PVDF) membrane (FFP73, Beyotime). The membranes were sealed with 5% skimmed milk for 1 h, followed by labeling with primary

antibodies: anti-WDPCP (AA179-228) (1:1000, ABIN6744036, Absin), anti-EMCN (1:1000, ab106100, Abcam), β-Actin (13E5) (1:2000, #4970, Cell Signaling Technologies), anti-E-cadherin (1:1500, ab231303, Abcam), anti-N-cadherin (1:1500, ab76057, Abcam) and anti-vimentin (1:1000, ab24525, Abcam) at 4°C for 24 h. After rinsing, the membranes were further probed using Horseradish peroxidase (HRP)-linked IgG: anti-rabbit IgG HRP (ab6721, 1:5000, Abcam) and goat anti-mouse IgG HRP (ab97023, 1:5000, Abcam) for 1 h. Western blot chemiluminescence kit (sc-2048) was utilized for protein band signal generation, and the developed bands were recorded using a GelDoc imaging system (Bio-Rad). Protein band intensities were quantified using Image J software (National Health Institute). β-Actin was used as the loading control of each sample. The intensity of each protein target band was normalized against that of β-Actin in each sample to determine the relative protein expression level.

Leucine level detection

Leucine levels in plasma samples were examined using the Leucine Level Detection Kit (BYP33468R, Baiyi Biotech). A total volume of 50 µL sample was processed with 250 µL of assay buffer and centrifuged at 12,500 g for 15 min. A 20 µL aliquot of the supernatant was added to each well of the assay plate, and the total sample volume was adjusted to 50 µL per well with assay buffer. To create a standard series, a 10 mM Leucine solution was diluted tenfold with dH$_2$O to produce a 1 mM Leucine sample. In the assay plate, standard series concentrations of 0, 2, 4, 6, 8, and 10 nmol were prepared from the 1 mM Leucine solution in 50 µL of assay buffer. The samples were then mixed with 50 µL of Reaction Mix and incubated for 30 min at 25°C. Optical density (OD) at 450 nm was measured using a microplate reader (Infinite 200 PRO; Tecan).

Enzyme-linked immunoassay (ELISA) analysis

The plasma levels of vascular endothelial growth factor A (VEGFA) and Angiopoietin-2 (Ang2) were measured using the VEGF-A Mouse ELISA Kit (#BMS619-2, Thermo Fisher Scientific) and the Mouse Angiopoietin 2 ELISA Kit (ab209883, Abcam), respectively. In brief, 20 µL of samples was diluted with 250 µL of assay buffer and centrifuged at 12,500 g for 15 min. Subsequently, 50 µL of the supernatant was added to the assay plate, and the samples were

incubated for 2 h at ambient temperature. After three rinses with the wash buffer, the samples were probed with a biotin-conjugated antibody for 1 h, followed by incubation with streptavidin-linked HRP reagent. After washing, 50 µL of the signal detection solution was added, and the samples were incubated in the dark for 30 min. The absorbance values were measured at 450 nm using a microplate reader (Infinite 200 PRO; Tecan). The quantity of each factor was determined using the serially diluted standards provided in each kit.

Phospho-MAPK and phospho-ERK measurement

Phospho-p38 MAPK and phospho-ERK levels were measured using the Human/Mouse/Rat Phospho-ERK1/2, JNK, p38 MAPK Cell-Based ELISA kit (#CBEL-ERK-SK, RayBiotech) and the ERK1/ERK2 (Phospho) Multispecies InstantOne™ ELISA Kit (#85-86013-11, ThermoFisher Scientific. A total of 50 µL of plasma or cell lysate was added to each well coated with capture antibody and incubated overnight at 4°C. Following this, the samples were washed and labeled with 100 µL of detection antibody for 1 h at 25°C. Subsequently, the samples were incubated with 50 µL of HRP-linked Anti-Rabbit or Mouse IgG for 1 h at 25°C. Color development was achieved using 100 µL of 3,3′,5,5′-Tetramethylbenzidine (TMB) reagent for 30 min. The reaction was then terminated with 50 µL of Stop Solution, and the absorbance was immediately measured at 450 nm. The phospho-protein-specific signal was normalized to the total protein content in each sample.

Animal model

C57BL/6J mice were obtained from Cyagen. The mice were raised at 22°C with a 12-h light-dark cycle and were given free access to regular chow. Eight-week-old pregnant females were assigned to different conditions ($n = 5$ animals per condition): 1. Control group: pregnant females were fed regular chow and provided with drinking water; 2. Model (High leucine) group: pregnant females were given drinking water containing 1.5% (weight/volume) L-leucine (MedChemExpress)[26,27]; 3. Model+WDPCP group: neonates from the model group were administered an adeno-associated virus (AAV) carrying the WDPCP expression fragment (prepared by Genewiz, Tianjin) via intravenous injection; 4. Model +C16-PAF group: neonates from the model group

received C16-PAF by intravenous injection at a dosage of 2.5 mg/kg every 3 days. The newborns were raised by the same female in each group. Tail blood collection was performed on week 2 from the newborns in each group. Left ventricular ejection fraction (LVEF) and fractional shortening (LVFS) were measured in neonatal mice (week 2) using a Vevo 3100 ultrasound system (FUJIFILM VisualSonics) with a 40 MHz MicroScan transducer (MS-550D). Mice were anesthetized with 1.5% isoflurane and positioned supine on a heated platform to maintain a body temperature of 37°C. M-mode echocardiography was conducted in the parasternal short-axis view at the level of the papillary muscle. Left ventricular internal dimensions were measured at end-diastole (LVIDd) and end-systole (LVIDs). LVFS was calculated using the formula: $(LVIDd - LVIDs)/LVIDd \times 100\%$. LVEF was derived using the Teichholz formula: $LVEF = (LVIDd^3 - LVIDs^3)/LVIDd^3 \times 100\%$. Three measurements were averaged for each parameter. Animal protocols complied with the guidelines for animal care and welfare and received approval from the Experimental Animal Ethics Committee of Yunnan Besta Biotechnology Co. LTD. (BST-MICE-20230505-01).

Epicardial adipose tissue volume (EATV) measurement

Two-week-old newborns were subjected to cardiac computed tomography (CT) for EATV measurement utilizing a 320-slice CT scanner (Aquilion One; Toshiba Medical Systems). The rotation time was set to 0.25 ms, and the collimation parameters were 0.5/320/0.25. Images were acquired in a non-helical, electrocardiogram-triggered mode with the following parameters: tube voltage of 120 kV, tube current of 400 mA for 5 ms, and slice thickness of 5 mm. The CT image data were analyzed using the Synapse Vincent workstation (Version 4.4, Fuji Film). EATV values were determined as previously described.[28]

Statistics

Statistical data analyses were conducted with SPSS software (version 20.0, IBM SPSS). All results were presented as the mean ± standard deviation. Two-group comparisons were performed using unpaired Student's t-tests, while multiple comparisons involving more than three conditions were assessed using one-way analysis of variance (ANOVA) followed by Tukey's post hoc test. A p-value of less than 0.05 was considered statistically significant.

RESULTS

Neonatal CHDs are associated with elevated plasma leucine levels and the dysregulation of WDPCP/EMCN axis

We initially collected blood samples from 10 healthy controls and 10 infants diagnosed with CHD. The analysis of leucine levels in the plasma revealed a significant elevation in CHD patients compared to healthy controls (Figure 1a, $p < 0.0001$). The protein levels of WDPCP and EMCN in the plasma samples were also analyzed by Western blot. The results demonstrated the downregulation of WDPCP and an increased expression of EMCN in the plasma of CHD patients (Figure 1b,c, $p < 0.05$ & $p < 0.01$). Given that the MAPK/ERK signaling pathway is implicated in CHD,[29,30] we further examined the activity of this pathway by detecting phosphorylated p38 and ERK levels in the plasma samples using ELISA. We observed suppressed phosphorylation levels of p38 and ERK in the plasma of CHD patients (Figure 1d,e, $p < 0.0001$). These data indicate that elevated leucine levels may affect CHD progression by regulating the MAPK/ERK signaling pathway and the WDPCP/EMCN axis, prompting us to investigate the roles of this signaling axis in cellular and animal models.

High-leucine diet in pregnant female mice triggers CHD-like features in the offspring

To demonstrate the direct effect of leucine on CHDs, we fed pregnant female mice a high-leucine diet to induce CHDs in their neonates. The neonates from the high-leucine diet model group exhibited a significantly higher level of leucine in plasma samples compared to the control group, which was fed a standard diet (Figure 2a, $p < 0.0001$). Additionally, 320-slice spiral CT analysis revealed a significant increase in EATV in the neonates from the model group (Figure 2b, $p < 0.0001$), indicating the onset of CHD. Furthermore, we observed a notable decrease in LVEF and left ventricular fractional shortening (LVFS) in the model group, suggesting impaired left ventricular function (Supporting Information S1: Figure S1A, $p < 0.05$). Meanwhile, there was a mild retardation in body weight gain observed in the high-leucine diet model group (Supporting Information S1: Figure S1B, $p < 0.05$).

We also measured the protein levels of WDPCP and EMCN and observed a decrease in WDPCP expression alongside an increase in EMCN levels in the neonatal
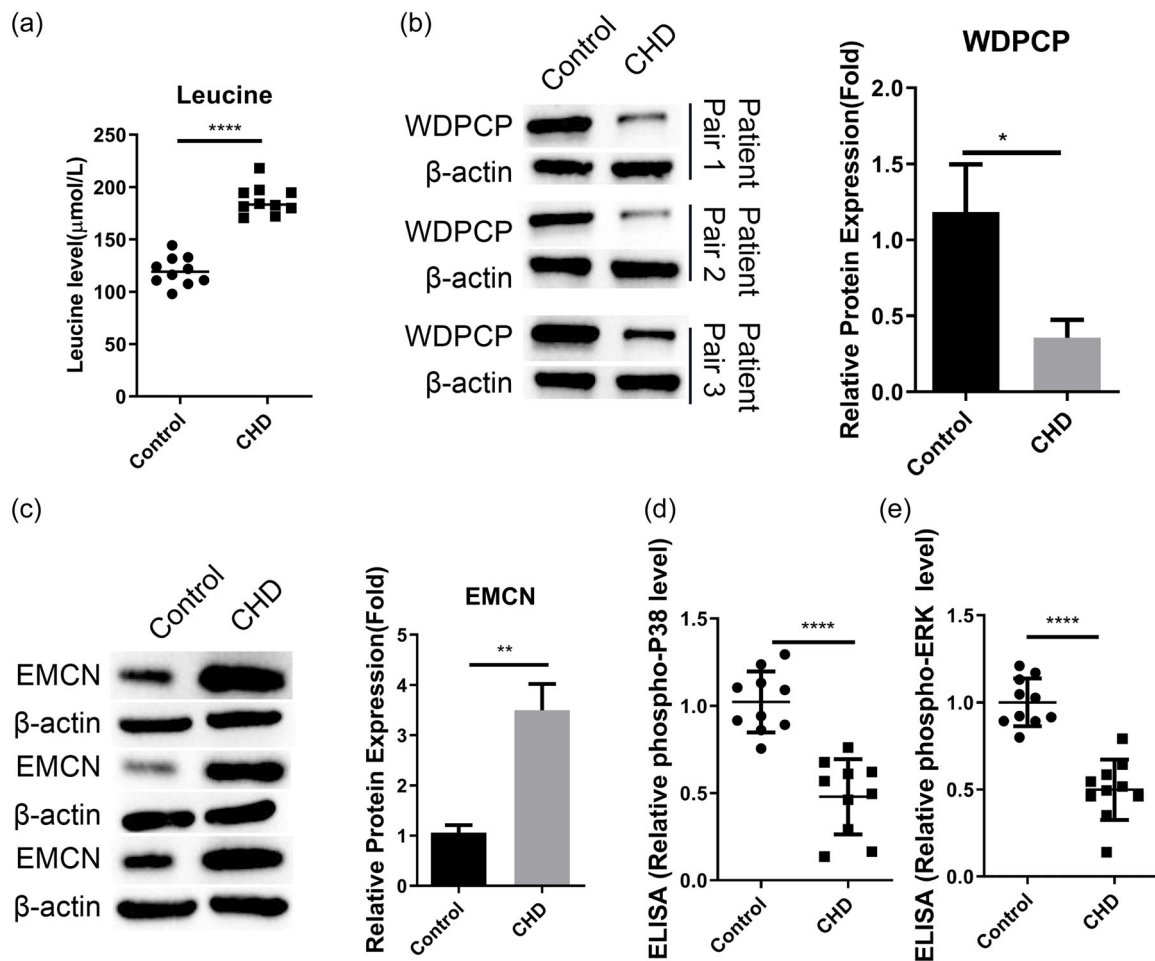
Pulmonary Circulation
Open Access

FIGURE 1 Neonatal CHDs are associated with elevated plasma leucine levels and dysregulation of the WDPCP/EMCN axis. (a) The analysis of leucine levels in plasma samples of healthy controls and neonatal CHD patients ($n = 10$ in each category). (b) Western blot analysis of the protein levels of WDPCP, and (c) EMCN in plasma samples of healthy controls and neonatal CHD patients ($n = 3$ in each category). (d) Detection of phospho-p38 and (e) phospho-ERK levels by ELISA in plasma samples of healthy controls and neonatal CHD patients ($n = 10$ in each category) were quantified ELISA. $*p < 0.05$; $**p < 0.01$; $***p < 0.001$; $****p < 0.0001$.

plasma of the model group (Figure 2c, $p < 0.001$). Concurrently, phosphorylation levels of p38 and ERK were found to be reduced in the plasma samples of neonates within the model group (Figure 2d,e, $p < 0.0001$). In contrast, the protein levels of VEGF-A and ANG2 were comparable between the control and model groups (Figure 2f, $p > 0.05$). These data suggest that elevated leucine levels in the plasma may influence the progression of CHDs through the MAPK/ERK signaling pathway and the WDPCP/EMCN axis. However, we did not observe significant changes in cardiac structure between the control and model groups (Figure 2g). These findings imply that a high-leucine diet may not impact cardiac development, but could affect certain physiological functions, such as those involving cardiac microvascular endothelial cells (HCMECs).

WDPCP overexpression and MAPK activator ameliorate high-leucine-induced CHDs

To evaluate the engagement of WDPCP and MAPK signaling in high-leucine-induced CHDs, neonates from the high-leucine diet model group were administered AAV for WDPCP overexpression or a MAPK activator (C16-PAF). Western blot analysis demonstrated a restoration of WDPCP expression and a reduction in EMCN levels in the plasma samples of the WDPCP overexpression group ($p < 0.0001$). In contrast, the MAPK activator did not influence WDPCP expression, although it did suppress EMCN levels (Figure 3a, $p < 0.0001$). Intriguingly, both WDPCP overexpression and MAPK activation were found to reduce EATV in the neonates of the high-leucine group, indicating an
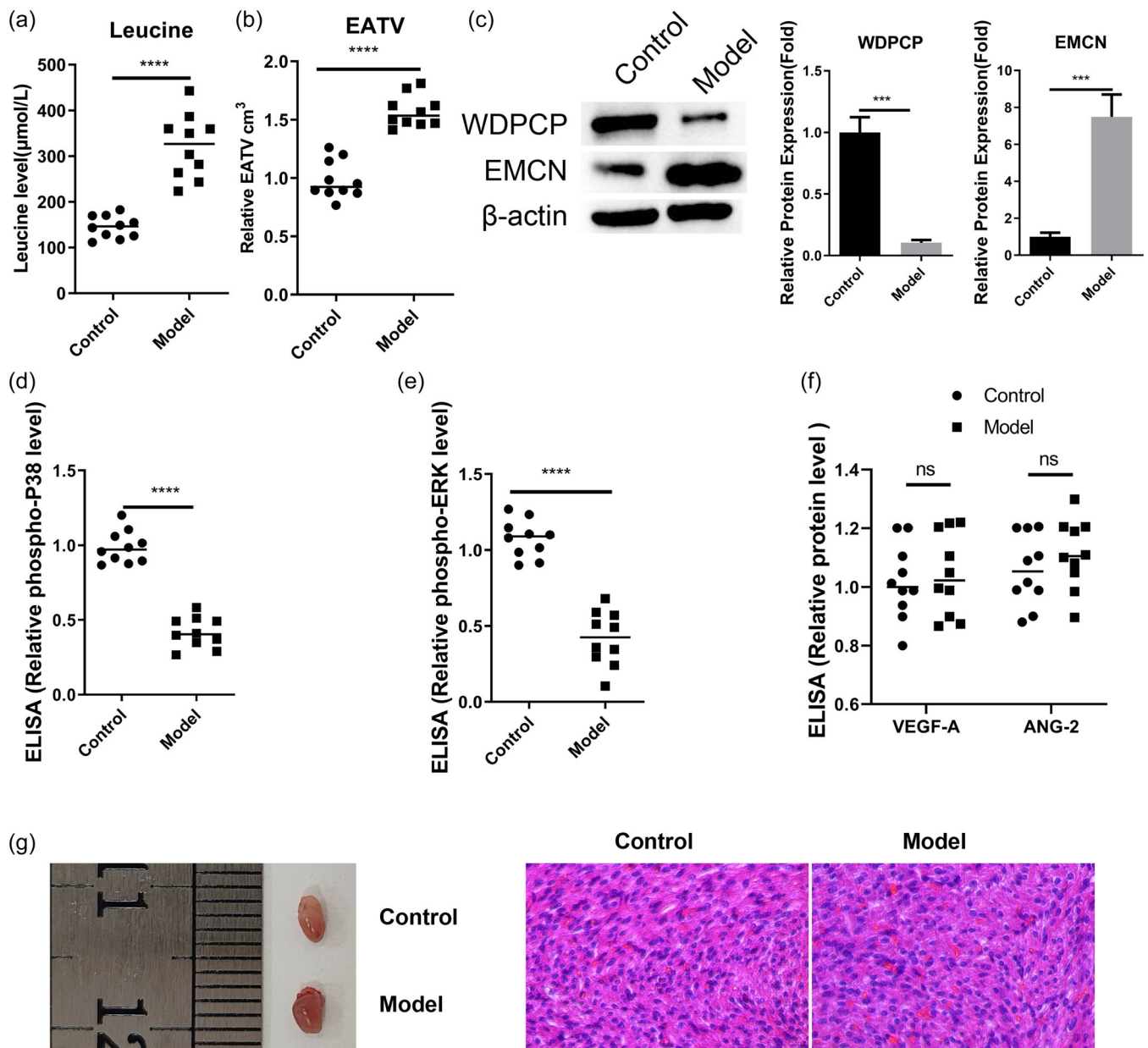
FIGURE 2 High-leucine diet in pregnant female mice triggers CHD-like features in the neonatal mice. Pregnant female mice ($n = 5$ in each group) were fed the standard diet or a high-leucine diet. (a) The plasma leucine levels were determined in the neonatal mice (2 weeks old) from the normal diet (control) and the high-leucine diet (model) groups. (b) 320-slice spiral CT analysis of epicardial adipose tissue volume (EATV) in neonatal mice from the control and model groups. (c) Analysis of WDPCP and EMCN protein expression in neonatal plasma samples of the control and model groups. (d) Detection of phospho-p38, and (e) phospho-ERK levels in plasma samples of neonatal mice from the the control and model groups. (f) Plasma VEGF-A and ANG2 levels were analyzed by ELISA in the control and model groups. (g) Hematoxylin & Eosin staining in the cardiac tissues of neonatal mice from the control and model groups. *$p < 0.05$; **$p < 0.01$; ***$p < 0.001$; ****$p < 0.0001$.

amelioration of CHDs (Figure 3b, $p < 0.01$ & $p < 0.001$). Further analysis of phospho-p38 and phospho-ERK levels revealed that both WDPCP overexpression and the MAPK activator enhanced the activity of MAPK/ERK signaling (Figure 3c,d, $p < 0.0001$). Therefore, the reduced WDPCP expression and impaired MAPK/ERK activity are implicated in high-leucine-induced CHDs. These findings also suggest that WDPCP acts as an upstream regulator of MAPK/ERK signaling, as WDPCP overexpression promoted phospho-p38 and phospho-ERK levels, while the MAPK activator had no effect on WDPCP expression.
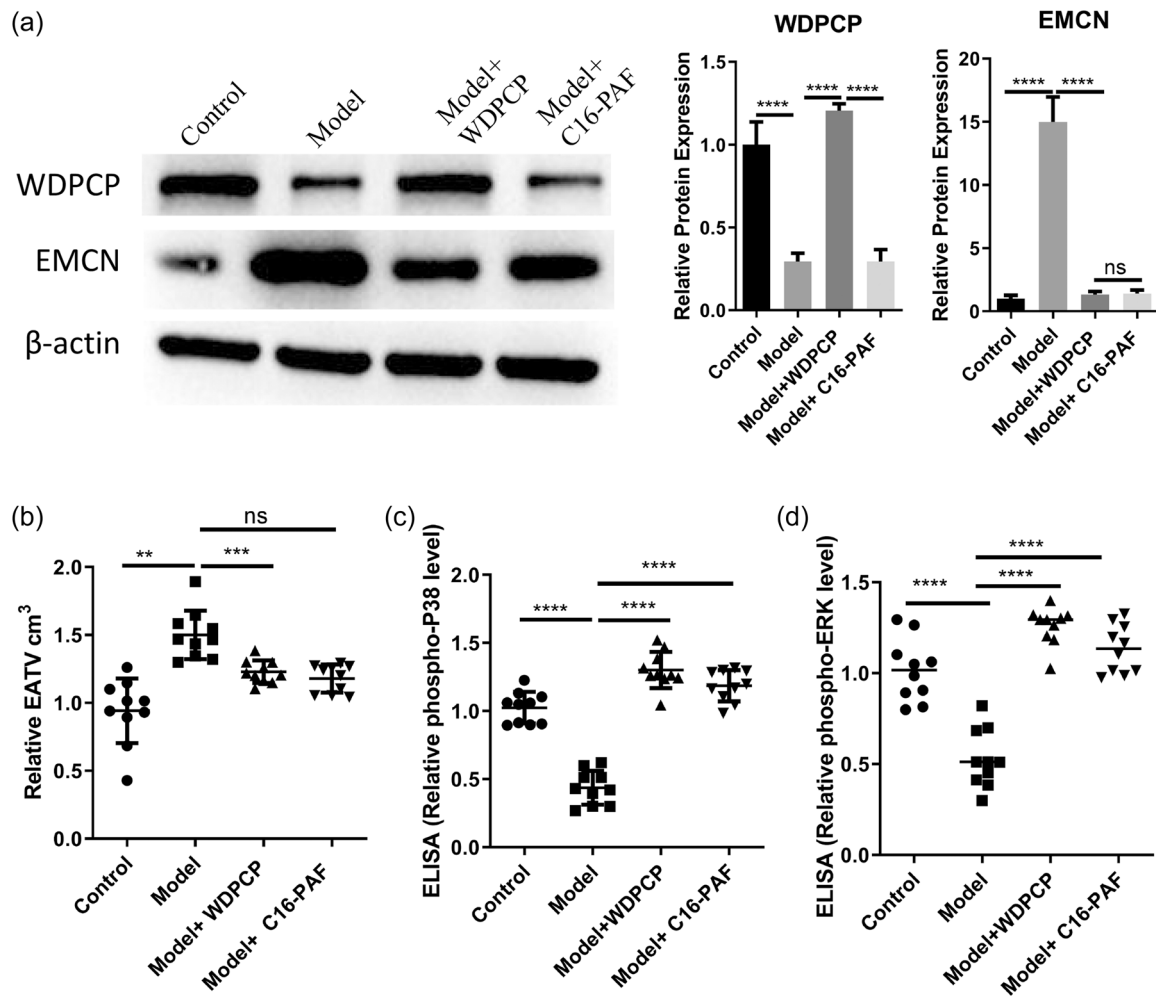
FIGURE 3 WDPCP overexpression and MAPK activation ameliorate high-leucine-induced CHDs. Pregnant female mice ($n = 5$ in each group) were fed the standard diet or a high-leucine diet. Neonatal mice from the high-leucine diet group was administered an AAV-carrying WDPCP expression construct or a MAPK signaling pathway activator (C16-PAF) for 2 weeks. (a) Western blot analysis of WDPCP and EMCN protein levels in plasma samples of the neonatal mice in each group. (b) 320-slice spiral CT analysis of epicardial adipose tissue volume (EATV) in the neonatal mice of each group. (c) Phospho-p38 and (d). phospho-ERK levels were examined in plasma samples of the neonatal mice by ELISA. $*p < 0.05$; $**p < 0.01$; $***p < 0.001$; $****p < 0.0001$. AAV, adeno-associated virus.

High-leucine levels regulate the WDPCP/EMCN axis and the MAPK/ERK signaling and impairs the EMT in HCMECs

To evaluate the influence of leucine on cardiac vascular cells, we utilized HCMECs as the cell model to investigate the effects of high leucine treatment (4 mM) on migratory ability and EMT status. We first examined the impact of elevated leucine levels on the WDPCP/EMCN axis and the MAPK/ERK signaling pathway. Compared to control cells cultured in standard medium (0.8 mM leucine), HCMECs in high-leucine medium (4 mM) exhibited reduced expression of WDPCP ($p < 0.001$) and increased levels of EMCN ($p < 0.0001$) (Figure 4a). Meanwhile, the levels of phospho-p38 and phospho-ERK were also diminished (Figure 4b,c, $p < 0.01$). These findings align with data

obtained from patient samples and animal models. Furthermore, high-leucine levels suppressed the migratory and invasive capacities of HCMECs (Figure 4d,e, $p < 0.001$). Given that the EMT process is involved in regulating cell mobility, we subsequently analyzed the expression levels of mesenchymal proteins (vimentin and N-cadherin) and the epithelial marker (E-cadherin). High-leucine treatment downregulated vimentin and N-cadherin expression while increasing E-cadherin protein levels (Figure 4f, $p < 0.01$, $p < 0.001$, or $p < 0.0001$). Thus, elevated leucine levels may suppress the expression of protein markers associated with EMT and impair the migratory ability of HCMECs. Notably, high-leucine levels did not significantly affect the proliferation of HCMECs (Figure 4g, $p > 0.05$), suggesting that the observed effects are not due to changes in cell growth.
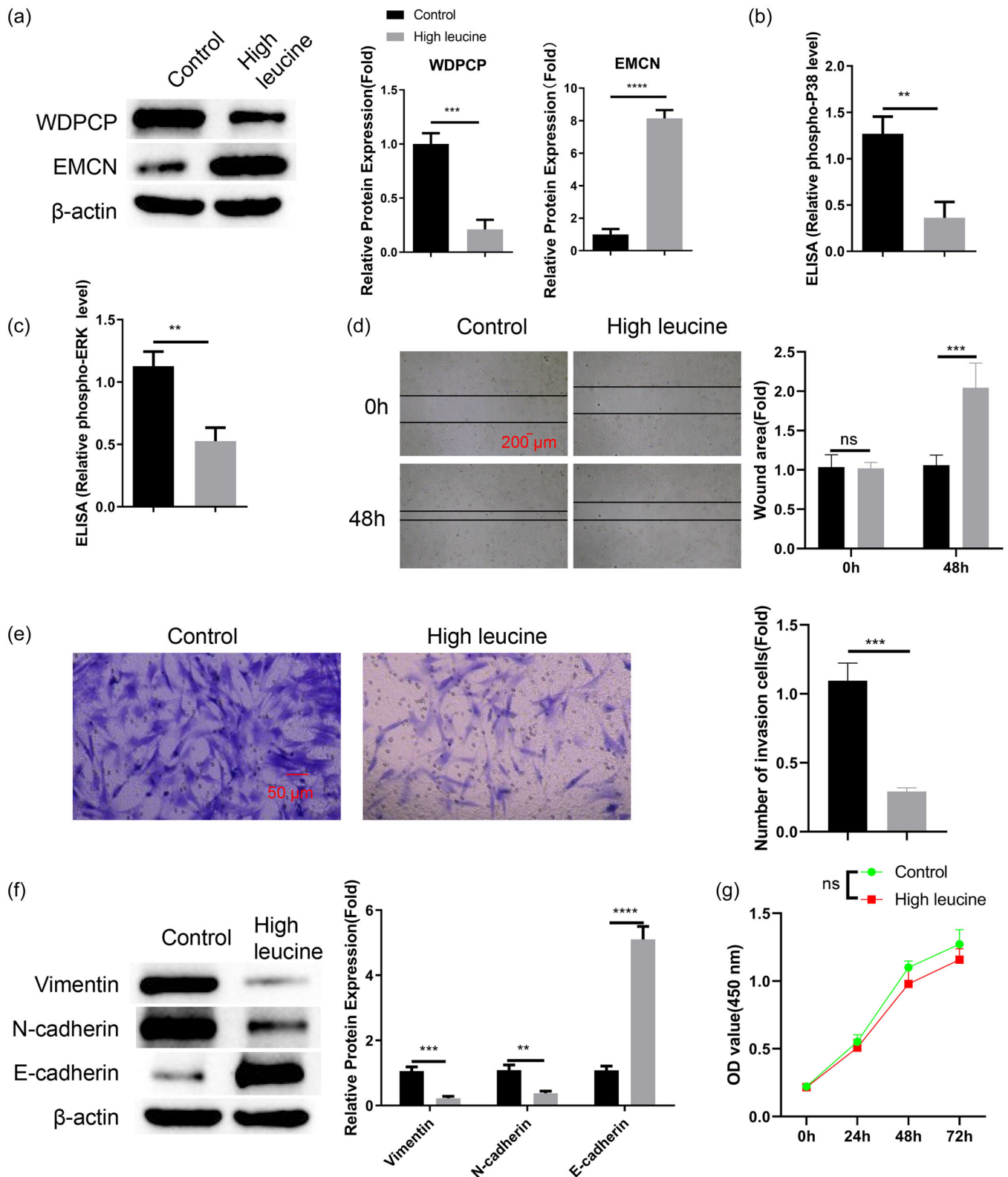
FIGURE 4 High-leucine levels regulate WDPCP/EMCN expression and the MAPK/ERK signaling, and impairs the EMT in HCMECs. HCMECs were cultured in standard medium (control, 0.8 mM) or high-leucine medium (4 mM) for 48 h. (a) Western blot analysis of WDPCP and EMCN levels in the control and high-leucine conditions. (b) Phospho-p38 and (c). phospho-ERK levels were examined in HCMECs cultured under the control and high-leucine conditions. (d) Wound healing assay and (e) transwell invasion assay in HCMECs cultured under the control and high-leucine conditions. (f) Western blot analysis of mesenchymal markers (vimentin and N-cadherin) and an epithelial marker (E-cadherin) in HCMECs cultured under the control and high-leucine conditions. (g) CCK-8 cell proliferation assay of HCMECs under the control and high-leucine culturing conditions. Data are the summary of three independent experiments. *$p < 0.05$; **$p < 0.01$; ***$p < 0.001$; ****$p < 0.0001$.

WDPCP and the MAPK signaling mediate the suppressive effect of high-leucine levels on cell migration and the EMT in HCMECs

We next aimed to investigate whether WDPCP and the MAPK signaling are implicated in high leucine level-induced suppression of cell mobility and the EMT. HCMECs cultured in a high leucine environment were transfected with a WDPCP overexpression plasmid or stimulated with a MAPK activator. Western blot analysis confirmed WDPCP overexpression in cells transfected with the WDPCP expression vector ($p < 0.0001$), and this over-expression also inhibited the upregulation of EMCN induced by high-leucine levels ($p < 0.0001$). Although the MAPK activator did not affect WDPCP expression, it did suppress EMCN expression ($p < 0.0001$) (Figure 5a).

Meanwhile, both WDPCP overexpression and the MAPK activator increased the levels of phospho-p38 and phospho-ERK (Figure 5b,c, $p < 0.0001$). Thus, these data further indicate that WDPCP levels govern the activity of MAPK/ERK signaling, which negatively regulates EMCN levels. Moreover, both WDPCP overexpression and the MAPK activator partially rescued cell migration and invasion in HCMECs cultured under high-leucine conditions (Figure 5d,e, $p < 0.001$). Consistently, the expression of mesenchymal proteins, such as vimentin and N-cadherin, was restored upon WDPCP overexpression or MAPK acti-vator treatment, while the high leucine-induced upregula-tion of E-cadherin was suppressed (Figure 5f, $p < 0.01$, $p < 0.001$, or $p < 0.0001$). Together, these findings imply that high-leucine levels impair mobility and the EMT process in HCMECs by repressing WDPCP expression and dampening the MAPK/ERK signaling.
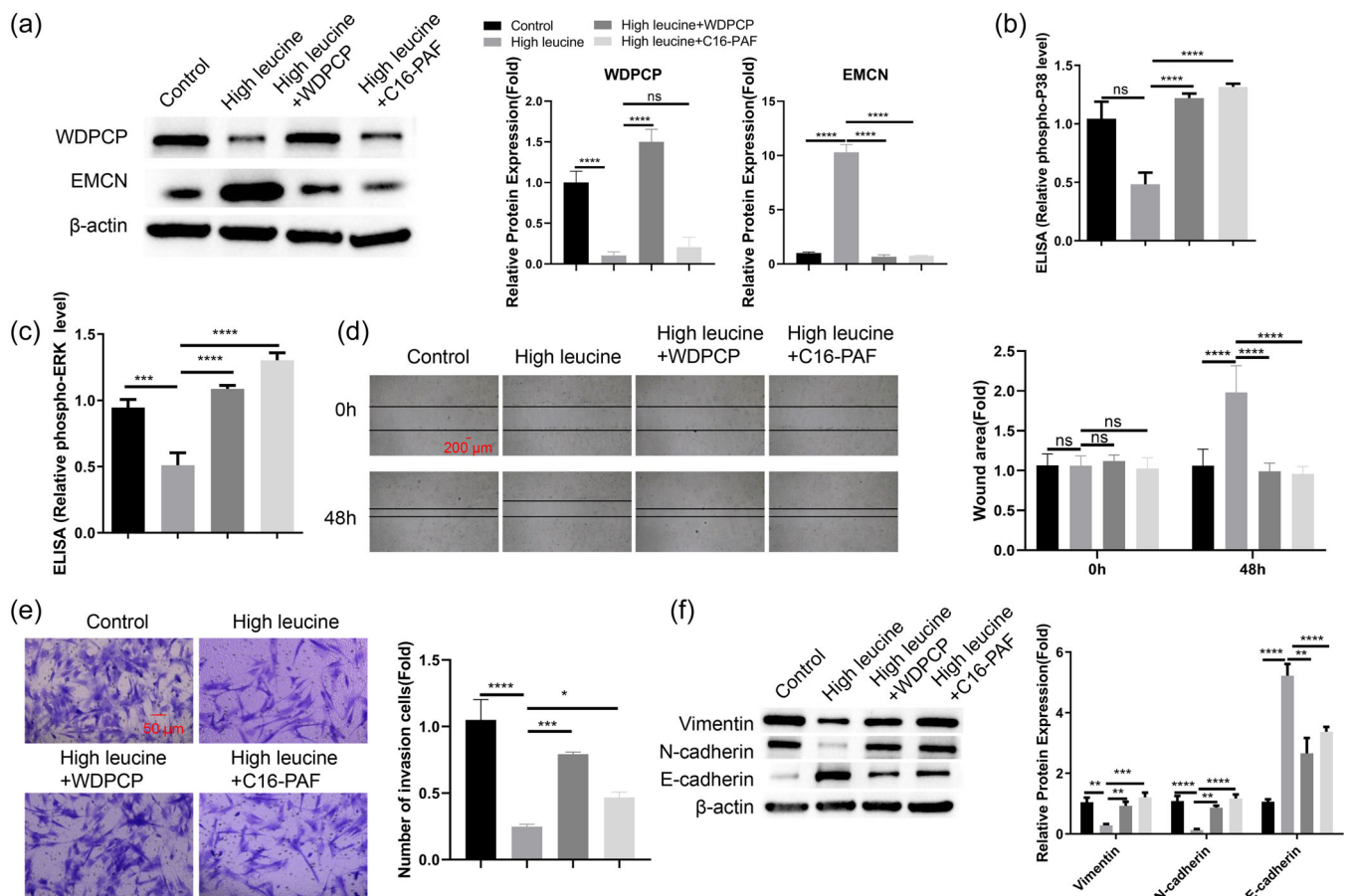

FIGURE 5 WDPCP and MAPK signaling mediates the suppressive effect of high-leucine levels on the EMT and cell migration in HCMECs. HCMECs transfected with a WDPCP expression vector or treated with the MAPK activator were cultured in standard medium (control) or high-leucine medium for 48 h. (a) Western blot analysis of WDPCP and EMCN levels in each experimental group. (b) Phospho-p38 and (c) phospho-ERK levels were examined in HCMECs of indicated experimental groups. (d) Wound healing assay and (e) transwell invasion assay in HCMECs of indicated experimental groups. (f) Western blot analysis of mesenchymal markers (vimentin and N-cadherin) and an epithelial marker (E-cadherin) in HCMECs of indicated experimental groups. Data are the summary of three independent experiments. *$p < 0.05$; **$p < 0.01$; ***$p < 0.001$; ****$p < 0.0001$.
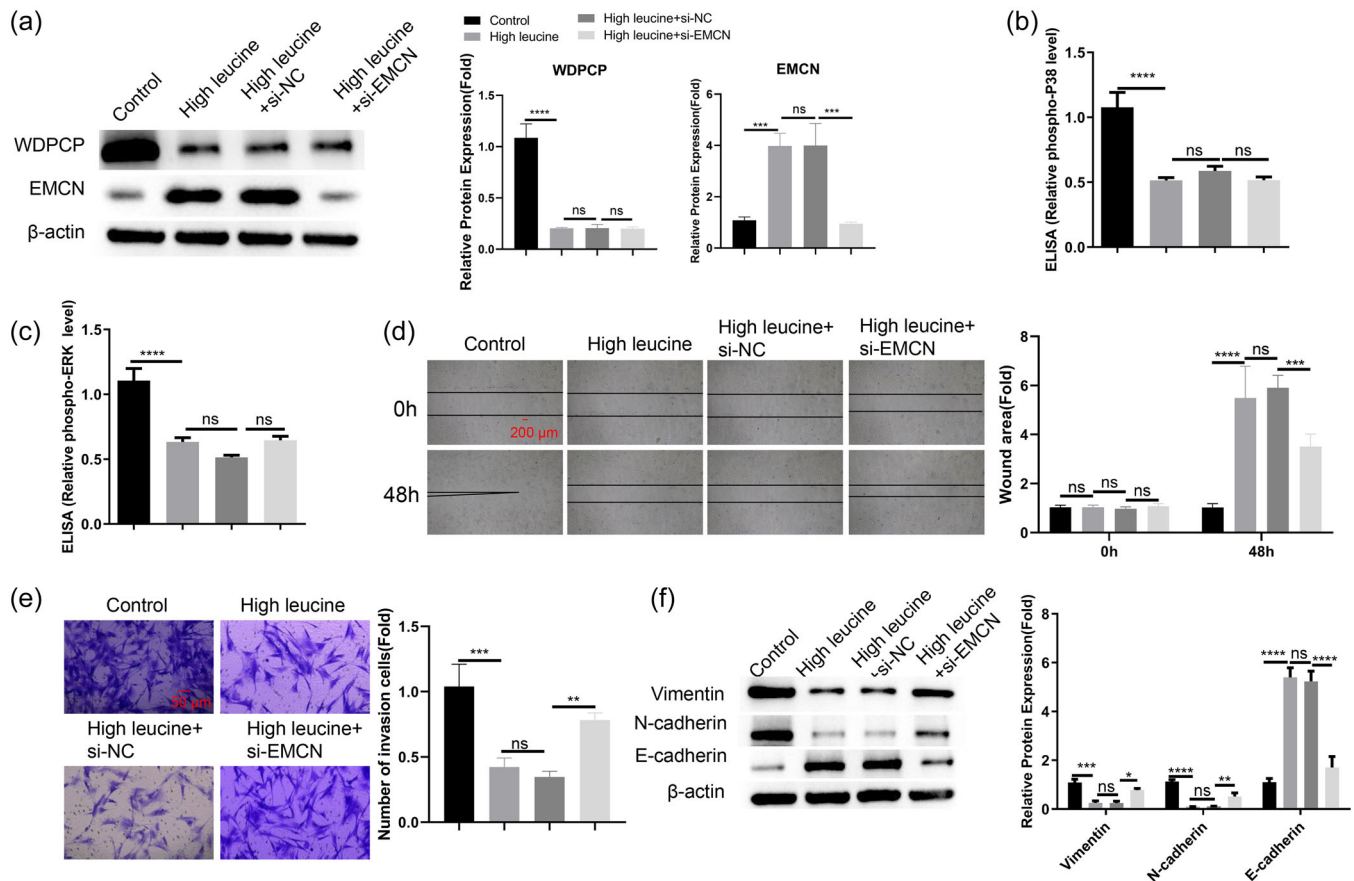
FIGURE 6 EMCN is a leucine-induced effector negativity regulating the EMT and migratory ability of HCMECs. HCMECs transfected with the control siRNA (si-NC) or an siRNA targeting EMCN (si-EMCN) were cultured in a standard medium (control) or high-leucine medium for 48 h. (a) Western blot analysis of WDPCP and EMCN levels in each experimental group. (b) Phospho-p38 and (c) phospho-ERK levels were examined in HCMECs of indicated experimental groups. (d) Wound healing assay and (e) transwell invasion assay in HCMECs of indicated experimental groups. (f) Western blot analysis of mesenchymal markers (vimentin and N-cadherin) and epithelial marker (E-cadherin) in HCMECs of indicated experimental groups. Data are the summary of three independent experiments. $*p < 0.05$; $**p < 0.01$; $***p < 0.001$; $****p < 0.0001$.

EMCN is a leucine-induced effector negativity regulating the EMT and migratory ability in HCMECs

Since EMCN is regulated by the WDPCP/MAKP/ERK axis, we next investigated whether EMCN serves as the effector that dictates the migratory ability and EMT in HCMECs. To this end, we applied siRNA targeting EMCN to knock down its expression in HCMECs treated with high levels of leucine. The application of EMCN siRNA effectively reduced EMCN levels under high leucine conditions ($p < 0.0001$), while the knockdown of EMCN did not affect WDPCP expression ($p > 0.05$) (Figure 6a). Furthermore, EMCN knockdown showed no significant effects on the levels of phospho-p38 and phospho-ERK (Figure 6b,c, $p > 0.05$). These findings further support the notion that EMCN acts as a downstream factor in the WDPCP/MAPK/ERK pathway.

Additionally, silencing of EMCN at least partially restored cell migration and invasion in HCMECs cultured under high-leucine levels (Figure 6d,e, $p < 0.001$). EMCN silencing also partially restored the levels of vimentin and N-cadherin, while reducing E-cadherin expression under high-leucine conditions (Figure 6f, $p < 0.05$, $p < 0.01$, or $p < 0.0001$). Collectively, these data indicate that EMCN is a downstream factor of the WDPCP/MAKP/ERK axis, and its overexpression under high-leucine conditions suppresses the migration and EMT of HCMECs.

DISCUSSION

The effects of maternal diet on CHDs have been extensively documented.[8-11] As essential components of a protein-rich diet, BCAAs are abundant in plasma and are

necessary for various metabolic and physiological functions related to heart development.[31] Dynamic changes in BCAA catabolism are implicated in cardiac development and cardiovascular disorders.[32] A deficiency in BCAA catabolism is associated with pathological remodeling of heart tissues, while excessive levels of BCAAs and their byproducts may contribute to the development of cardiovascular diseases.[33,34] In this study, we report that plasma samples from neonatal CHD patients exhibited elevated levels of leucine. Furthermore, we demonstrated that dietary leucine supplementation in pregnant female mice could induce CHD-like features in their offspring. These findings align with a previous report indicating that increased gestational leucine levels in plasma correlate with a heightened risk of CHDs.[15] Additionally, it is noteworthy that long-term leucine supplementation can lead to growth retardation in breast-fed piglets[35] and impair exercise-induced cardiovascular adaptations in rats.[36] Therefore, maintaining a balanced dietary intake of leucine is essential for normal fetal development.

We also revealed that WDPCP, a protein implicated in planar cell polarity signaling and collective cell movement,[16] was reduced in the plasma samples of CHD patients and in neonatal mice from the high-leucine diet group. High-leucine treatment in HCMECs similarly decreased WDPCP expression. Planar cell polarity signaling plays a crucial role in the angiogenic organization of endothelial cells, arterial remodeling, and heart morphogenesis.[18–21] Disruption of endothelial cell polarity impairs both endothelial angiogenesis and cardiac septation.[37,38] Additionally, disruption of planar cell polarity can lead to cardiomyocyte disorganization in CDH.[39] WDPCP has been reported to mediate epicardial EMT and cardiac cell migration during coronary artery remodeling.[22] Consistent with this, our findings indicate that high-leucine-induced downregulation of WDPCP suppresses EMT and the migration of HCMECs. The impaired EMT and migration may be attributed to WDPCP's role as a regulator of endothelial cell polarity, which warrants further investigation. Furthermore, the mechanism by which high-leucine levels suppress WDPCP expression requires future clarification.

Intriguingly, the overexpression of WDPCP can reduce the volume of epicardial adipose tissue (EATV) in neonatal mice from the high-leucine diet group. The accumulation of EAT is associated with cardiac arrhythmias.[40] A previous study indicates that the epicardium contains multipotent cells capable of differentiating into adipocytes through epicardium-mesenchymal transformation.[41] Therefore, future studies are necessary to clarify whether WDPCP regulates the transition of epicardium to adipocytes by modulating the EMT process.

The MAPK/ERK signaling pathway is crucial for regulating endothelial function and coronary artery remodeling.[29,30] Our research demonstrated that this pathway is attenuated in patients with CHDs, as well as in neonatal mice from the high-leucine diet group and high-leucine-treated HCMECs. The administration of a MAPK activator mitigates the adverse effects of elevated leucine levels in both animal and cell models. Notably, our findings further revealed that WDPCP serves as an upstream regulator of the MAPK/ERK signaling, as its overexpression enhanced the levels of phospho-p38 and phospho-ERK, while the MAPK activator did not affect WDPCP levels. It is well established that cytoskeletal dynamics and cell polarity signaling can regulate MAPK signaling activity.[42–44] Therefore, the influence of WDPCP on MAPK/ERK signaling may be attributed to its role in regulating cytoskeletal organization.[16]

We further reported that EMCN functions as a downstream effector that negatively regulates the EMT and cell migration in HCMECs. EMCN is significantly induced by high levels of leucine treatment, and its knockdown partially rescues the EMT status and migratory ability of HCMECs under high-leucine conditions. These results align with a previous study indicating that EMCN suppresses VEGF-induced endothelial cell migration, growth, and morphogenesis.[45] Another study suggests that EMCN disrupts focal adhesion assembly and abolishes the interaction between cells and the extracellular matrix.[46] However, its role in cardiac function and development remains largely unexplored. Although we demonstrated that its expression can be attenuated by WDPCP overexpression or MAPK activation, further research is necessary to clarify how the WDPCP/MAPK signaling axis regulates EMCN expression.

While this study provides valuable insights into the role of high leucine levels in the development of CHDs through the WDPCP/MAPK/ERK/EMCN axis, several limitations and areas for future research remain. Firstly, the partial restoration of cellular functions upon EMCN knockdown suggests the involvement of additional pathways or factors that are not explored in this study. Future research should aim to identify these potential contributors through comprehensive pathway analyses or unbiased omics approaches. To fully understand the effects of high leucine treatment on HCMECs, it is recommended to consider RNA-seq or proteomics analysis. These high-throughput techniques could reveal a broader spectrum of molecular changes and potentially identify novel targets or pathways involved in leucine-induced CHDs. Secondly, the precise mechanism by which leucine affects WDPCP expression remains unclear. Further investigation into the molecular interactions between leucine and WDPCP, possibly involving leucine sensors

or metabolic regulators, could shed light on this aspect. Additionally, the study primarily focused on cardiac microvascular endothelial cells, and the effects of high leucine levels on other cardiac cell types should be examined to provide a more comprehensive understanding of CHD development. The long-term consequences of elevated gestational leucine levels on cardiac function and structure in offspring beyond the neonatal period also warrant investigation. Finally, translating these findings into potential therapeutic strategies for preventing or mitigating CHD risk in high-risk pregnancies represents an important future direction. Such strategies could involve dietary interventions, targeted modulation of the WDPCP/MAPK/ERK pathway, or approaches to regulate EMCN expression in developing cardiac tissues.

CONCLUSIONS

Taken together, our data indicate that elevated plasma leucine levels are associated with neonatal CHDs. High-leucine levels reduce WDPCP expression and dampen the signaling activity of the MAPK/ERK axis in both animal and cell models, resulting in the overexpression of EMCN. EMCN upregulation impairs the EMT and the migratory capacity of cardiac microvascular endothelial cells. These findings suggest that excessive leucine intake in pregnant females and newborns increases the risk of neonatal CHDs, highlighting the potential of targeting the WDPCP/MAPK axis as an intervention strategy.

CONFLICT OF INTEREST STATEMENT
The authors declare no conflicts of interest.

ETHICS STATEMENT
The acquisition of all clinical materials had been approved by the Medical Ethics Committee of Kunming Children's Hospital (2021-03-340-K01). In addition, all the recruited subjects had provided informed consent. All the sample handling and data processing steps were following the Declaration of Helsinki. Animal protocols were in compliance with the guidelines of animal care and welfare and were approved by the Experimental Animal Ethics Committee of Yunnan Besta Biotechnology Co. LTD. (BST-MICE-20230505-01).

ORCID
Jian Chen http://orcid.org/0009-0004-7270-3730

REFERENCES

1. Tennant PW, Pearce MS, Bythell M, Rankin J. 20-year survival of children born with congenital anomalies: a population-based study. Lancet. 2010;375(9715):649–56.

2. Martin GR, Schwartz BN, Hom LA, Donofrio MT. Lessons learned from infants with late detection of critical congenital heart disease. Pediatr Cardiol. 2022;43(3):580–5.

3. Eckersley L, Sadler L, Parry E, Finucane K, Gentles TL. Timing of diagnosis affects mortality in critical congenital heart disease. Arch Dis Child. 2016;101(6):516–20.

4. Bolin EH, Gokun Y, Romitti PA, Tinker SC, Summers AD, Roberson PK, Hobbs CA, Malik S, Botto LD, Nembhard WN. Maternal smoking and congenital heart defects, national birth defects prevention study, 1997–2011. J Pediatr. 2022;Jan 240: 79–86.e1.

5. Bateman BT, Patorno E, Desai RJ, Seely EW, Mogun H, Dejene SZ, Fischer MA, Friedman AM, Hernandez-Diaz S, Huybrechts KF. Angiotensin-converting enzyme inhibitors and the risk of congenital malformations. Obstet Gynecol. 2017;129(1):174–84.

6. Wu Y, Reece EA, Zhong J, Dong D, Shen WB, Harman CR, Yang P. Type 2 diabetes mellitus induces congenital heart defects in murine embryos by increasing oxidative stress, endoplasmic reticulum stress, and apoptosis. Am J Obstet Gynecol. 2016;215(3):366.e1–366.e10.

7. Levy HL, Guldberg P, Güttler F, Hanley WB, Matalon R, Rouse BM, Trefz F, Azen C, Allred EN, De La Cruz F, Koch R. Congenital heart disease in maternal phenylketonuria: report from the maternal PKU collaborative study. Pediatr Res. 2001;May 49(5):636–42.

8. Yang J, Kang Y, Cheng Y, Zeng L, Shen Y, Shi G, Liu Y, Qu P, Zhang R, Yan H, Dang S. Iron intake and iron status during pregnancy and risk of congenital heart defects: a case-control study. Int J Cardiol. 2020;301:74–9.

9. Mao B, Qiu J, Zhao N, Shao Y, Dai W, He X, Cui H, Lin X, Lv L, Tang Z, Xu S, Huang H, Zhou M, Xu X, Qiu W, Liu Q, Zhang Y. Maternal folic acid supplementation and dietary folate intake and congenital heart defects. PLoS One. 2017;12(11):e0187996.

10. Yang J, Kang Y, Cheng Y, Zeng L, Yan H, Dang S. Maternal dietary patterns during pregnancy and congenital heart defects: a case-control study. Int J Environ Res Public Health. 2019;16(16):2957.

11. Abqari S, Gupta A, Shahab T, Rabbani M, Ali S, Firdaus U. Profile and risk factors for congenital heart defects: a study in a tertiary care hospital. Ann Pediatr Cardiol. 2016;9(3):216–21.

12. Toneto AT, Ferreira Ramos LA, Salomão EM, Tomasin R, Aereas MA, Gomes-Marcondes MCC. Nutritional leucine supplementation attenuates cardiac failure in tumour-bearing cachectic animals. J Cachexia Sarcopenia Muscle. 2016;Dec 7(5):577–86.

13. Grajeda-Iglesias C, Aviram M. Specific amino acids affect cardiovascular diseases and atherogenesis via protection against macrophage foam cell formation: review article. Rambam Maimonides Med J. 2018;9(3):e0022.

14. Fidale TM, Antunes HKM, Alex Dos Santos L, Rodrigues de Souza F, Deconte SR, Borges Rosa de Moura F, Mantovani MM, Alves Duarte PR, Roever L, Resende ES. Increased dietary leucine reduces Doxorubicin-associated cardiac dysfunction in rats. Front Physiol. 2018;8:1042.

15. Zhang X, Liu L, Chen WC, Wang F, Cheng YR, Liu YM, Lai YF, Zhang RJ, Qiao YN, Yuan YY, Lin Y, Xu W, Cao J, Gui YH, Zhao JY. Gestational leucylation suppresses

embryonic T-box transcription factor 5 signal and causes congenital heart disease. Adv Sci. 2022;9(15):e2201034.

16. Cui C, Chatterjee B, Lozito TP, Zhang Z, Francis RJ, Yagi H, Swanhart LM, Sanker S, Francis D, Yu Q, San Agustin JT, Puligilla C, Chatterjee T, Tansey T, Liu X, Kelley MW, Spiliotis ET, Kwiatkowski AV, Tuan R, Pazour GJ, Hukriede NA, Lo CW. Wdpcp, a PCP protein required for ciliogenesis, regulates directional cell migration and cell polarity by direct modulation of the actin cytoskeleton. PLoS Biol. 2013;11(11):e1001720.

17. Langhans MT, Gao J, Tang Y, Wang B, Alexander P, Tuan RS. Wdpcp regulates cellular proliferation and differentiation in the developing limb via hedgehog signaling. BMC Dev Biol. 2021;21(1):10.

18. Li D, Wang J. Planar cell polarity signaling in mammalian cardiac morphogenesis. Pediatr Cardiol. 2018;39(5):1052–62.

19. Merks AM, Swinarski M, Meyer AM, Müller NV, Özcan I, Donat S, Burger A, Gilbert S, Mosimann C, Abdelilah-Seyfried S, Panáková D. Planar cell polarity signalling coordinates heart tube remodelling through tissue-scale polarisation of actomyosin activity. Nat Commun. 2018;9(1):2161.

20. Cirone P, Lin S, Griesbach HL, Zhang Y, Slusarski DC, Crews CM. A role for planar cell polarity signaling in angiogenesis. Angiogenesis. 2008;11(4):347–60.

21. Wang C, Qu K, Wang J, Qin R, Li B, Qiu J, Wang G. Biomechanical regulation of planar cell polarity in endothelial cells. Biochimica et Biophysica Acta (BBA) - Molecular Basis of Disease. 2022;1868(12):166495.

22. Liu X, Wang Y, Liu F, Zhang M, Song H, Zhou B, Lo CW, Tong S, Hu Z, Zhang Z. Wdpcp promotes epicardial EMT and epicardium-derived cell migration to facilitate coronary artery remodeling. Sci Signal. 2018;11(519):eaah5770.

23. Cagle SD, Cooperstein N. Coronary artery disease. Primary Care: Clin Office Pract. 2018;45(1):45–61.

24. Joloudari JH, Hassannataj Joloudari E, Saadatfar H, Ghasemigol M, Razavi SM, Mosavi A, Nabipour N, Shamshirband S, Nadai L. Coronary artery disease diagnosis; ranking the significant features using a random trees model. Int J Environ Res Public Health. 2020;17(3):731.

25. She P, Van Horn C, Reid T, Hutson SM, Cooney RN, Lynch CJ. Obesity-related elevations in plasma leucine are associated with alterations in enzymes involved in branched-chain amino acid metabolism. Am J Physioly-Endocrinol Metab. 2007;293(6):E1552–63.

26. Zhao Y, Dai X, Zhou Z, Zhao G, Wang X, Xu M. Leucine supplementation via drinking water reduces atherosclerotic lesions in apoEnull mice. Acta Pharmacol Sin. 2016;37(2):196–203.

27. Zhang Y, Guo K, LeBlanc RE, Loh D, Schwartz GJ, Yu YH. Increasing dietary leucine intake reduces diet-induced obesity and improves glucose and cholesterol metabolism in mice via multimechanisms. Diabetes. 2007;56(6):1647–54.

28. Maimaituxun G, Yamada H, Fukuda D, Yagi S, Kusunose K, Hirata Y, Nishio S, Soeki T, Masuzaki H, Sata M, Shimabukuro M. Association of local epicardial adipose tissue depots and left ventricular diastolic performance in patients with preserved left ventricular ejection fraction. Circ J. 2020;84(2):203–16.

29. Jie L, Yong-Xiao C, Zu-Yi Y, Cang-Bao X. Minimally modified LDL upregulates endothelin type B receptors in rat coronary artery via ERK1/2 MAPK and NF-κB pathways. Biochim Biophys Acta (BBA) - Mol Cell Biol Lipids. 2012;1821(4):582–9.

30. Valanti EK, Dalakoura-Karagkouni K, Fotakis P, Vafiadaki E, Mantzoros CS, Chroni A, Zannis V, Kardassis D, Sanoudou D. Reconstituted HDL-apoE3 promotes endothelial cell migration through ID1 and its downstream kinases ERK1/2, AKT and p38 MAPK. Metabolism. 2022;127:154954.

31. Latimer MN, Sonkar R, Mia S, Frayne IR, Carter KJ, Johnson CA, Rana S, Xie M, Rowe GC, Wende AR, Prabhu SD, Frank SJ, Rosiers CD, Chatham JC, Young ME. Branched chain amino acids selectively promote cardiac growth at the end of the awake period. J Mol Cell Cardiol. 2021;157:31–44.

32. Tobias DK, Mora S, Verma S, Lawler PR. Altered branched chain amino acid metabolism: toward a unifying cardiometabolic hypothesis. Curr Opin Cardiol. 2018;33(5):558–64.

33. Xiong Y, Jiang L, Li T. Aberrant branched-chain amino acid catabolism in cardiovascular diseases. Front Cardiovasc Med. 2022;9:965899.

34. Sun H, Wang Y. Branched chain amino acid metabolic reprogramming in heart failure. Biochim Biophys Acta (BBA) - Mol Basis Dis. 2016 Dec;1862(12):2270–5.

35. Ji Y, Sun Y, Liu N, Jia H, Dai Z, Yang Y, Wu Z. L-leucine supplementation reduces growth performance accompanied by changed profiles of plasma amino acids and expression of jejunal amino acid transporters in breast-fed intra-uterine growth-retarded piglets. Br J Nutr. 2022;129:1–33.

36. Dos Santos GB, de Oliveira AG, Ramos LAF, Gomes-Marcondes MCC, Areas MA. Long-term leucine supplementation aggravates prolonged strenuous exercise-induced cardiovascular changes in trained rats. Exp Physiol. 2016;101(7):811–20.

37. Li D, Angermeier A, Wang J. Planar cell polarity signaling regulates polarized second heart field morphogenesis to promote both arterial and venous pole septation. Development. 2019;146(20):dev181719.

38. Patel NR, R K C, Blanks A, Li Y, Prieto MC, Meadows SM. Endothelial cell polarity and extracellular matrix composition require functional ATP6AP2 during developmental and pathological angiogenesis. JCI Insight. 2022;7(19):e154379.

39. Phillips HM, Rhee HJ, Murdoch JN, Hildreth V, Peat JD, Anderson RH, Copp AJ, Chaudhry B, Henderson DJ. Disruption of planar cell polarity signaling results in congenital heart defects and cardiomyopathy attributable to early cardiomyocyte disorganization. Circ Res. 2007;101(2):137–45.

40. Ernault AC, Verkerk AO, Bayer JD, Aras K, Montañés-Agudo P, Mohan RA, Veldkamp M, Rivaud MR, de Winter R, Kawasaki M, van Amersfoorth SCM, Meulendijks ER, Driessen AHG, Efimov IR, de Groot JR, Coronel R. Secretome of atrial epicardial adipose tissue facilitates reentrant arrhythmias by myocardial remodeling. Heart Rhythm. 2022;(9):1461–70.

41. Yamaguchi Y, Cavallero S, Patterson M, Shen H, Xu J, Kumar SR, Sucov HM. Adipogenesis and epicardial adipose tissue: a novel fate of the epicardium induced by mesenchymal transformation and PPARγ activation. Proc Natl Acad Sci. 2015;112(7):2070–5.

42. Pullikuth A, Catling A. Scaffold mediated regulation of MAPK signaling and cytoskeletal dynamics: a perspective. Cell Signal. 2007;19(8):1621–32.

43. Zhang Y, Wang P, Shao W, Zhu JK, Dong J. The BASL polarity protein controls a MAPK signaling feedback loop in asymmetric cell division. Dev Cell. 2015;33(2):136–49.

44. Samaj J. From signal to cell polarity: mitogen-activated protein kinases as sensors and effectors of cytoskeleton dynamicity. J Exp Bot. 2003;55(395):189–98.

45. Park-Windhol C, Ng YS, Yang J, Primo V, Saint-Geniez M, D'Amore PA. Endomucin inhibits VEGF-induced endothelial cell migration, growth, and morphogenesis by modulating VEGFR2 signaling. Sci Rep. 2017;7(1):17138.

46. Kinoshita M, Nakamura T, Ihara M, Haraguchi T, Hiraoka Y, Tashiro K, Noda M. Identification of human endomucin-1 and -2 as membrane-bound O-sialoglycoproteins with anti-adhesive activity. FEBS Lett. 2001;499(1–2):121–6.

SUPPORTING INFORMATION

Additional supporting information can be found online in the Supporting Information section at the end of this article.